Coastal Engineering 190 (2024) 104507

Contents lists available at ScienceDirect

Coastal Engineering

journal homepage: www.elsevier.com/locate/coastaleng

On the onset of pipeline scouring: Reconciling waves and currents forcing

Francesco Marini [a,*], Matteo Postacchini [a], Claudia Pizzigalli [b], Maurizio Badalini [b], Sara Corvaro [a], Maurizio Brocchini [a]

[a] Department of Construction, Civil Engineering and Architecture, Università Politecnica delle Marche, via Brecce Bianche 12, Ancona, 60131, AN, Italy
[b] SAIPEM SpA, Italy

ARTICLE INFO

Keywords:
Waves
Currents
Onset
Scour
KC
Pipeline

ABSTRACT

The combined action of waves and currents can lead to the generation of freespans that have significant influence on both pipeline on-bottom stability and structural integrity. Several studies have been carried out since the 80's to analyse the onset of the scour process and the related phenomena in the presence of either waves or currents, while only a few studies regard the combination of waves and currents. Moreover, the main empirical expressions coming from such studies cannot adequately represent the physics of the phenomena and lead to non-conservative results. For that purpose, a reanalysis of existing datasets on the onset of scour due to waves and/or currents has been carried out to obtain a coherent method for the evaluation of the critical embedment associated to such mixed flow conditions. In addition, an analytical study has been used to quantify the *Keulegan–Carpenter* parameter when waves are combined with currents, for a more correct application of such empirical formulas. These results will be integrated into a probabilistic model for the long-time evolution of freespans for the evaluation of the structural stability of pipelines in the marine environment, although the present approach can be exploited for a broader range of offshore applications that deal with the combined action of waves and currents.

1. Introduction

Submarine pipelines are offshore key infrastructures widely used for long-distance transportation of oil and gas from production wells to processing facilities. Furthermore, underwater pipes and cables are also related to the growing use of renewable energy sources and to the consequent development of dedicated offshore structures for the energy harvesting from diverse sources (e.g., wind, waves, sun). Their integrity is influenced by a large number of factors. An uneven seabed, with respect to a flat one, leads to the generation of freespans that can lead to an increase of the bending stress in the unsupported sections. A similar effect can be generated also by dynamic phenomena such as the migration of submerged bars, which are subjected to both short-term and long-term evolution (e.g. Pape et al., 2010; Postacchini et al., 2017; Melito et al., 2020; Grossmann et al., 2022; Pourzangbar and Brocchini, 2022), as well as the submarine formation of "sand waves". These are large-scale seabed forms whose presence can hamper the integrity of pipelines also because of their migration (e.g. Besio et al., 2003, 2004). The type of soil can lead to other problems: a hard soil (e.g. rock) is related to the abrasion of the pipeline, a soft soil (e.g. clay) can lead to an excessive sinking of the pipeline inside it. Finally, the combined action of waves and currents can lead to the generation of freespans that have a significant influence on the pipeline on-bottom stability and structural integrity.

Since the 80's, a large amount of literature on pipelines in marine environment has been produced as reviewed by Fredsøe (2016). Most of those works focused on the scour development in terms of equilibrium scour depth and the related time scale either in waves (Sumer and Fredsøe, 1990; Hansen, 1992; Zhang et al., 2019), currents (Bijker and Leeuwestein, 1984; Chiew, 1991; Kjeldsen et al., 1973; Mao, 1986; Moncada-M and Aguirre-Pe, 1999) and their combination (Lucassen, 1984; Cheng et al., 2014; Zhang et al., 2017; Zang et al., 2019). In steady currents, when a pipeline is embedded into the seabed, the seepage flow caused by the presence of a drop of pressure between the upstream/downstream sides of the pipe can lead to the onset of scouring (Mao, 1986). The experimental study of Chiew (1990) related the scour onset to the process of piping by applying different static pressure gradients on the pipe. However, such works did not provide any quantification of the effect of the pressure drop in the soil. The first expression for the evaluation of the onset conditions was obtained by Sumer et al. (1991) for waves. The critical embedment of the pipeline was found to be related to the *Keulegan–Carpenter* (KC) parameter, as also confirmed by Klomp et al. (1995). The first work for

* Corresponding author.
E-mail address: f.marini@staff.univpm.it (F. Marini).

https://doi.org/10.1016/j.coastaleng.2024.104507
Received 9 May 2023; Received in revised form 6 March 2024; Accepted 18 March 2024
Available online 19 March 2024

waves or current flows alone was done by Sumer et al. (2001). Their results confirmed that the onset of the scour below pipelines occurs locally due to the piping caused by the excessive seepage flow. The critical condition for the scour to occur both in waves and currents was also obtained as a relation between a dimensionless flow velocity and the relative pipeline embedment, with a minor influence of the pipe *Reynolds* number and surface roughness. In the case of waves only, KC is a very important parameter for the onset conditions. Large values of KC lead to smaller pressure drops and flow separation occurs farthest from the pipe, thus recalling the steady current flow. On the contrary, given the same wave velocity, small values of KC are related to shorter waves, thus inducing larger pressure drops on the sides of the pipeline. Therefore, for small values of KC the onset conditions are easier to achieve.

More recently, the onset of scouring in steady current and waves was also studied numerically (Liang and Cheng, 2005; Zang et al., 2009). In Zang et al. (2009), a 2D-RANS model with a $k-\omega$ turbulence closure was developed to obtain a unified onset condition for steady currents and waves, which relates the dimensionless flow velocity defined in Sumer et al. (2001) to the critical embedment, the pressure drop coefficient and KC (in case of waves). The only work that analyzes the onset of scour under the combined action of waves and currents is the experimental study of Zang et al. (2010). Here, the critical velocity under waves and currents was defined from the interpolation of the results obtained by application of the equation of Zang et al. (2009) for steady currents. It was observed that such critical velocity is slightly larger in the combined flow and reaches the maximum value when current and wave velocities are comparable.

The main loads that must be considered when designing a pipeline are permanent (seabed roughness), functional (internal pressure and temperature) and dynamic (marine currents and direct wave action). Pipe-soil interaction and scouring are responsible of freespan generation (Bijker et al., 1991), whose effects on the pipelines mainly depend on the equilibrium depth and length. However, an accurate knowledge on scour onset conditions is very relevant, e.g. for oil & gas companies, to plan field maintenance operations. Real time data on scour, sagging and on the general pipeline status are often unavailable. For this reasons, companies use numerical/measured meteorological data (waves and currents) and experimental equations to estimate if scouring and freespans are expected or not (Drago et al., 2015). From this point of view, knowing the conditions leading to freespan generation in an environment where both waves and current coexist is essential to plan maintenance activities. Therefore, the aim of the present work is to revise the available methods for the evaluation of the onset of scour conditions under waves and currents, and to provide a uniform and updated approach that can be applied also when their action is combined.

The present work is structured as follows. In Section 2, a reanalysis of the main available methods for the evaluation of the onset of scour conditions at a pipeline is performed. In Section 3, the new model for the determination of the onset of scour is presented and validated with experimental data, together with the analysis of the main flow parameters in waves plus currents conditions. Finally, in Section 4, a discussion of the method and some conclusions are given to provide a useful framework for its application.

2. Re-analysis of the available methods

To characterize the onset of scouring under pipelines, most of the literature link the relative embedment of the pipeline (e/D, where e is the pipe embedment or burial depth and D is the pipe diameter) to a dimensionless ratio (Ω in the present work) between the squared critical velocity of the flow u_{crit} and some characteristics of both sediment and pipeline: the specific weight $s = \rho_s/\rho_w$ defined as the ratio between the sediment (ρ_s) and water density (ρ_w), the porosity n and D. The criterion for the onset of scour can, thus, be written in the following general form:

$$\Omega = \frac{u_{crit}^2}{gD(s-1)(1-n)} = f\left(\frac{e}{D}\right) \tag{1}$$

where g is gravity acceleration.

It must be noted that, in this equation, an important parameter for the sediment mobility, the mean grain size d_{50}, is missing. In his review on the interaction between a pipeline and an erodible bed, Fredsøe (2016) refers to the work of Zang et al. (2010) for the evaluation of the onset of piping conditions under combined waves and currents. In such work, the relation between the critical pipeline embedment and the flow conditions was taken from the numerical work of Zang et al. (2009) as:

$$\Omega = \frac{u_{crit}^2}{gD(s-1)(1-n)} = \frac{\gamma}{\lambda_a \Delta C_{p0}} \tag{2}$$

γ is the contact angle, which can be computed as a function of the dimensionless critical embedment as:

$$\gamma = 2\arccos\left(\frac{0.5-e/D}{0.5}\right). \tag{3}$$

ΔC_{p0} is the pressure drop coefficient across the pipeline size, which can be obtained from Figure 10 in Zang et al. (2010), and λ_a is a calibrating coefficient given by the relationship:

$$\lambda_a = 3\exp(-0.42\gamma). \tag{4}$$

In Zang et al. (2010), a new definition of the critical velocity was given:

$$u_{crit}^2 = \frac{(u_c+u_w)^2}{\beta} \tag{5}$$

where u_c and u_w are the sea current and wave velocities perpendicular to the pipeline, respectively. The ratio between the current velocity and the sum of the velocities is here defined as:

$$\alpha = \frac{u_c}{u_c+u_w} \tag{6}$$

From such coefficient, β was experimentally fitted as:

$$\beta = -2.6208\alpha^2 + 2.7417\alpha + 0.8396. \tag{7}$$

The first step of our analysis consists in the evaluation of Zang et al. (2010)'s approach in relation to the onset of scouring data for waves and currents available in the literature (Sumer et al., 2001; Zang et al., 2010). The ranges of the main parameters of the experimental tests of such works are reported in Table 1.

The application of the Zang et al. (2010)'s approach to such dataset leads to the results illustrated in Fig. 1. Here, the dimensionless critical embedment computed by inverting Eq. (2) is provided on the abscissa and the experimental data is reported on the ordinate. In the current only condition, the method of Zang et al. (2010) corresponds to Zang et al. (2009)'s approach and its validity is confirmed with the experimental data of Sumer et al. (2001) (red triangles). When the wave velocity increases (green squares) the performance of the approach is reduced down to the situation in which the flow is induced by waves only (blue circles). In this case, the critical embedment observed by experimental data can be orders of magnitude larger than the predictions from Eq. (2), characterized by a non-conservative behaviour.

In Drago et al. (2007), for combined waves and current environment, the equations given in Sumer et al. (2001) are applied for scour onset estimation depending on the value of α to establish if the flow is current dominated ($\alpha > 0.5$) or wave dominated ($\alpha < 0.5$), and to compute the combined value of the velocity to be used in the equation. The application of this approach would lead to discontinuity on the results at $\alpha = 0.5$ and to possible under/overestimation of the critical embedment in the other cases.

For this reason, the aim of the present work is to provide a uniform method for the evaluation of the critical embedment that leads to the

Table 1
Datasets used in the present study and relative range of the main parameters.

Authors	Type	D (m)	u_c (m/s)	u_w (m/s)	KC (–)	d_{50} (mm)	e/D (–)
Sumer et al. (2001)	Current	0.05–0.10	0.22–0.73	–	–	0.18–1.25	0.01–0.15
Sumer et al. (2001)	Waves	0.05–0.10	–	0.09–0.40	2.2–29.0	0.18	0.01–0.15
Zang et al. (2010)	Waves + current	0.05	0.13–0.45	0.07–0.36	1.6–48.0	0.16–0.48	0.03–0.15

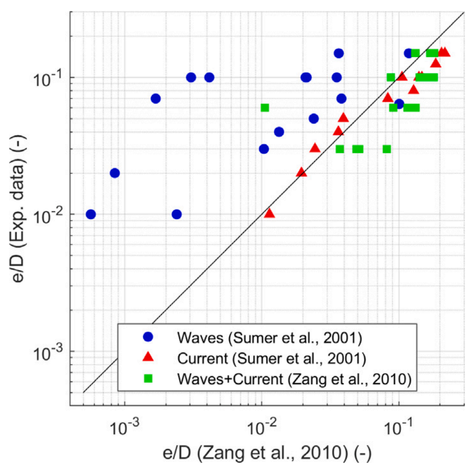

Fig. 1. Application of the onset evaluation method proposed by Zang et al. (2010) to wave plus current dataset of Zang et al. (2010) (in green) and the wave (in blue) and current (in red) datasets of Sumer et al. (2001).

onset of scour under combined waves and current, also in relation to the datasets available in the literature and reported in Table 1. The most validated approach on this topic that separately deals with waves and currents is that by Sumer et al. (2001). In the current only condition, an equation is provided to relate the current velocity with both sediment and pipeline characteristics as:

$$\Omega = \frac{u_{crit}^2}{gD(s-1)(1-n)} = 0.025 \exp\left(9\left(\frac{e}{D}\right)^{0.5}\right) \tag{8}$$

In the wave only condition, the dependence on the *Keulegan–Carpenter* number ($KC = u_w T/D$, where T is the wave period) is highlighted, but no explicit equation that accounts for its effect was provided and only a qualitative graph was reported (Figure 12 of Sumer et al., 2001). For a given wave velocity, smaller values of KC are related to smaller wave periods and, therefore, to larger values of the critical embedment, due to the increase of the pressure gradient between the two sides of the pipeline. On the opposite, for larger values of KC, the critical value of $\frac{u_{crit}^2}{gD(s-1)(1-n)}$ approaches the case of steady currents. Fig. 2 illustrates the performances of both Eq. (8) for the current only condition (panel *a*) and Figure 12 of Sumer et al. (2001) for the wave only condition (panel *b*). Eq. (8) agrees well with the experimental results of both critical embedment and dimensionless velocity, and provides a coefficient of determination $r^2 = 0.873$ (Fig. 2a). In the case of waves, Fig. 2b shows the experimental values of the dimensionless parameter Ω on the ordinate with respect to the values that can be obtained from Sumer et al. (2001)'s graph as a function of KC and of the dimensionless embedment. The results show an overall good agreement with the experimental values but the correlation is weaker with respect to the current only case ($r^2 = 0.573$). Such weaker correlation can be due to the fact that KC may not be the only parameter that influences the wave-induced piping process. The scatter plot of Fig. 3 highlights the importance of both KC and Shields parameter (θ), computed for wave tests only. According to Sumer et al. (2001), the dimensionless velocity is reported as a function of the dimensionless embedment. First, as also stated by Sumer et al. (1991), KC highly influences the onset of scour process under waves. Specifically, waves with large values of KC are characterized by large wave-lengths and their behaviour becomes closer and closer to that of steady currents for increasing KC (Fig. 3a). Then, another important parameter is found to highly influence the onset of scour in waves, i.e. the Shields parameter, whose effect is illustrated in Fig. 3b. When θ increases, the results for wave tests become similar to those of the steady current case. Here, the Shields parameter under waves is computed according to the associated wave shear stress (Shields, 1936) as:

$$\theta_w = \frac{\tau_w}{\rho g(s-1)d_{50}} \tag{9}$$

where the wave shear stress is computed as:

$$\tau_w = \rho u_{*w}^2 \tag{10}$$

while the friction velocity in waves is calculated as:

$$u_{*w} = \sqrt{\frac{f_w}{2}} u_w \tag{11}$$

and the friction coefficient is estimated according to Fredsoe and Deigaard (1992) as:

$$f_w = 0.04\left(\frac{a_x}{2.5d_{50}}\right)^{-\frac{1}{4}} \tag{12}$$

with a_x representing the amplitude of particle motion under waves.

3. The scour onset model

The new approach for the definition of an unique method for the evaluation of the onset of scour under combined waves and currents starts from the results of Sumer et al. (2001) for steady currents. Eq. (8) represents the relationship between the critical embedment of the pipeline and the critical velocity of the flow (Fig. 2a). Such equation can be, thus, modified to include also the important contribution of the Shields parameter when waves are dominating the flow. It can, thus, be rewritten introducing two coefficients, a and b, that depend on KC and θ as:

$$\Omega = \frac{u_{crit}^2}{gD(s-1)(1-n)} = a(KC,\theta) \exp\left(9\left(\frac{e}{D}\right)^{b(KC,\theta)}\right). \tag{13}$$

In practical applications, this model can be applied to obtain the critical embedment associated to specific flow, soil and pipeline conditions. From Eq. (13), the critical embedment can be obtained as:

$$\frac{e}{D} = \left[\frac{1}{9}\ln\left(\frac{u_{crit}^2}{agD(s-1)(1-n)}\right)\right]^{\frac{1}{b}} \tag{14}$$

If the pipeline embedment is smaller than the embedment computed with Eq. (14), the scour onset conditions are reached and the scour process occurs. To apply such model, the argument of the logarithm in Eq. (14) must be larger than 1. This condition is reached when the critical velocity increases to values larger than:

$$u_{crit} \geq \sqrt{agD(s-1)(1-n)} \tag{15}$$

Eq. (15) represents the condition for scour onset to occur when the pipeline embedment is null. The same condition was also present in Eq. (8), for steady currents, with $a = 0.025$. In waves only, the scour onset conditions are more easily reached due to the larger pressure gradient on the sides of the pipeline. A smaller value of such critical velocity is, thus, expected.

To apply the present model to the data reported in Zang et al. (2010), the value of s was taken as 2.65 and the porosity n was

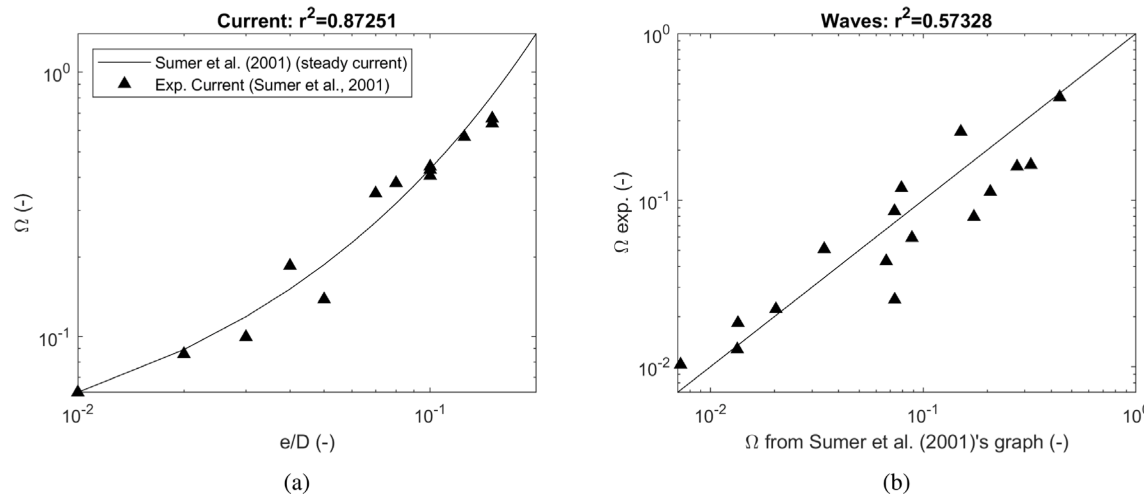

Fig. 2. Currents only condition (panel a): comparison between experimental values of Ω (triangles) and data computed with Eq. (8) (line) as a function of the dimensionless embedment. Waves only condition (panel b): experimental values of Ω vs. Ω computed from the graph of Sumer et al. (2001) as a function of the dimensionless embedment and of KC.

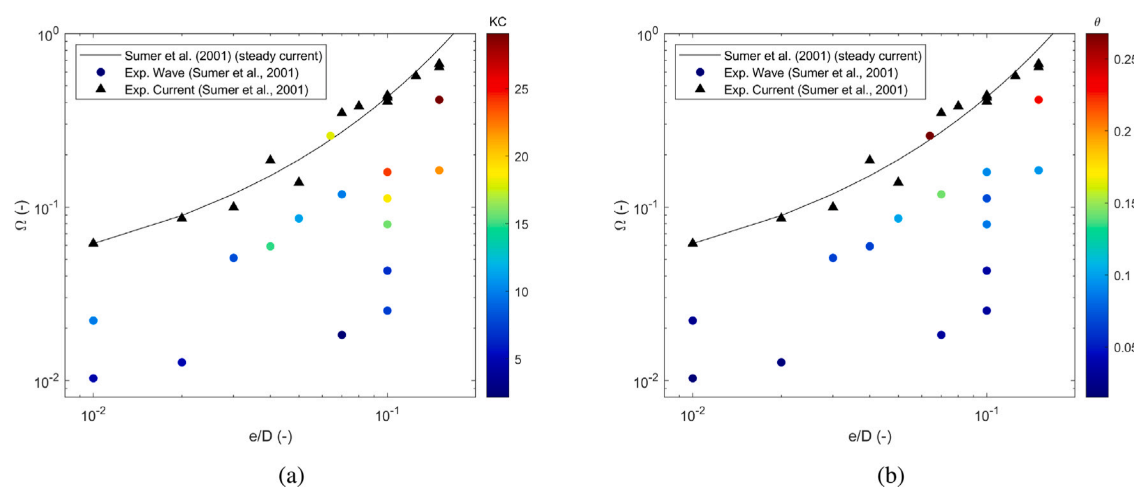

Fig. 3. Influence of the KC number (panel a) and of the Shields parameter (panel b) on the scour onset under a pipeline. The colorbar refers to wave tests only.

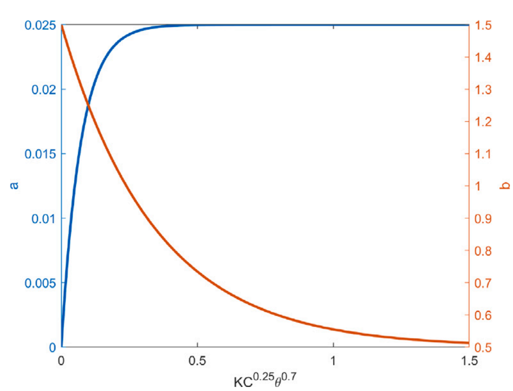

Fig. 4. Evolution of the parameters a and b defined in Eq. (17) as a function of the parameter $KC^{0.25}\theta^{0.70}$.

estimated from the grain size, according to Wu and Wang (2006) as:

$$n = 0.13 + \frac{0.21}{\left(1000 d_{50} + 0.002\right)^{0.21}} \tag{16}$$

The experimental data suggests an exponential behaviour for both a and b, depending on the combined parameter $KC^{0.25}\theta^{0.70}$. After substituting such exponential behaviours in Eq. (13), data fitting on the experimental values of Ω allowed us to obtain the following equations:

$$\begin{aligned} a &= 0.025\left(1 - \exp\left(-14KC^{0.25}\theta^{0.70}\right)\right) \\ b &= 0.5 + \exp\left(-2.9KC^{0.25}\theta^{0.70}\right) \end{aligned} \tag{17}$$

The exponential curves of Eq. (17) are plotted in Fig. 4. The asymptotic analysis of such equations is consistent with the expected behaviour of these parameters. An increase of the combined parameter $KC^{0.25}\theta^{0.70}$, due to large values of KC or θ, leads to a behaviour comparable to that of a current (see Fig. 3). In agreement with this consideration, for large values of $KC^{0.25}\theta^{0.70}$, the parameter a tends to 0.025 and b to 0.5, this providing Eq. (8) of Sumer et al. (2001) is obtained. Values of $KC^{0.25}\theta^{0.70} \rightarrow 0$ are mainly obtained by a zero velocity and, therefore, also a approaches 0 because no critical embedment can be associated with a zero velocity.

The present method can now be applied to the experimental data of Sumer et al. (2001) for either waves or currents. In detail, for its application in the wave only condition, the KC parameter is computed according to its definition as $KC = u_w T/D$ and the Shields parameter according to Eq. (9). For the current only condition, the value of KC is taken to be infinity and the Shields parameter is computed

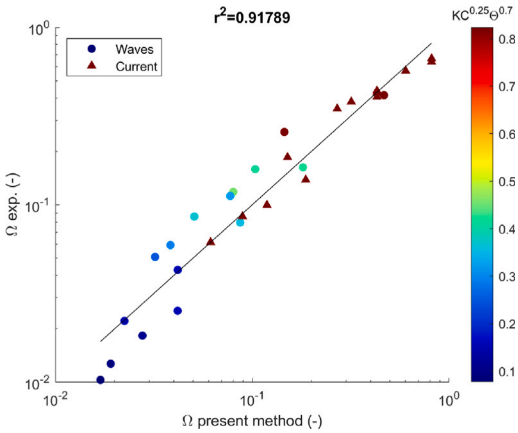

Fig. 5. Application of Eq. (13) to the onset data for either waves or current only conditions of Sumer et al. (2001).

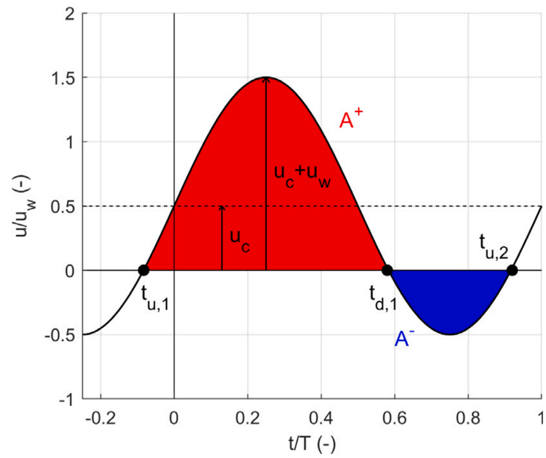

Fig. 6. Definition of the forward (A^{+}) and backward (A^{-}) particle excursion in case of combined waves and current velocity.

following Soulsby (1997) as follows. First, the current friction velocity is computed assuming a logarithmic velocity profile as:

$$u_{*c} = \kappa u_c(z) \ln\left(\frac{z_0}{z}\right) \quad (18)$$

where z is the level at which the current velocity is known, $\kappa = 0.41$ is the von Karman's constant, while the bed roughness length z_0 can be estimated according to Nikuradse (1932) as $z_0 = 2.5d_{50}/30$. Following the same procedure described for waves, the current shear stress can, thus, be computed as:

$$\tau_c = \rho u_{*c}^2 \quad (19)$$

and the associated Shields mobility parameter as:

$$\theta_c = \frac{\tau_c}{\rho g(s-1)d_{50}}. \quad (20)$$

The present approach is now applied to the experimental results of Sumer et al. (2001). Fig. 5 shows the results for the dimensionless parameter Ω. Here, the ordinate gives the experimental values while the abscissa gives the results achieved by application of the present method. The present approach represents very well the experimental data: coefficient of determination $r^2 = 0.918$ is obtained, which is larger than the coefficients obtained using Sumer et al. (2001)'s approach for waves/currents illustrated in Fig. 2. Eq. (13) is, therefore, validated with experimental data from tests of either waves or current only. However, it can also be applied to the cases in which waves and currents occur at the same time. For such application, some additional considerations are needed about the definition of the main parameters in combined waves and currents conditions. In particular, the following parameters are discussed in the following subsections:

- the Shields parameter
- the *Keulegan–Carpenter* number
- the critical velocity for the onset of scouring

3.1. θ For combined waves and currents

The significant amount of nonlinear interactions between wave and current boundary layers can enhance by 50% the maximum shear stress (Soulsby et al., 1993), which is found to be larger than the simple linear addition of τ_c and τ_w. Following Soulsby (1997), the maximum shear stress (τ_{max}) for combined waves and currents is computed from the mean shear stress defined as:

$$\tau_m = \tau_c \left[1 + 1.2\left(\frac{\tau_w}{\tau_c + \tau_w}\right)^{3.2}\right] \quad (21)$$

This equation was calibrated with laboratory and field data and accounts for the nonlinearity introduced by the interaction between waves and current. From this value, the maximum shear stress can be calculated by a vectorial sum of τ_m and τ_w according to Ockenden and Soulsby (1994) as:

$$\tau_{max} = \left[(\tau_m + \tau_w \cos\phi)^2 + (\tau_w \sin\phi)^2\right]^{0.5} \quad (22)$$

where ϕ is the relative angle between waves and current. The Shields parameter for combined waves and currents can now be computed, according to its definition, as:

$$\theta = \frac{\tau_{max}}{\rho g(s-1)d_{50}} \quad (23)$$

According to Zhang et al. (2017), the Shields parameter computed following this procedure is the one that better represents the time scale of the scour process under combined waves and current and it is, therefore, used in the present work.

3.2. KC For combined waves and current

The other main parameter that needs to be defined in combined waves and current conditions is the KC number. Its importance in the interaction with cylindrical structures was first shown by Keulegan and Carpenter (1958) who defined such dimensionless parameter as:

$$KC = \frac{u_w T}{D} = \frac{\pi A}{D} \quad (24)$$

being A the distance that a fluid particle would travel in the horizontal direction in the absence of the cylinder.

This definition can only be applied for a wave-induced motion in the surroundings of the pipeline. When a steady current is superimposed to the wave velocity field, the resultant velocity would be of the type:

$$u(t) = u_c + u_w \sin(\omega t) \quad (25)$$

where $\omega = 2\pi/T$ is the wave angular frequency and t is time. This leads to an increase of the excursion in the forward direction of the flow (A^{+}) and to a decrease in the backward direction (A^{-}). The two horizontal distances can be computed as the time integral of the positive and negative velocities of the flow, respectively. A sketch for this integration is illustrated in Fig. 6. Here, three specific time instants can be identified:

- the first up-crossing time $t_{u,1}$: it is zero when no current is present and moves to negative values up to $-T/4$ when $u_c \to u_w$
- the down-crossing time $t_{d,1}$: it is equal to $T/2$ without current and grows up to $3/4T$ when $u_c \to u_w$
- the following up-crossing time $t_{u,2}$: it is equal to T without the superimposed current and it decreases to $3/4T$ when $u_c \to u_w$. In this situation, $t_{d,1} \approx t_{u,2}$.

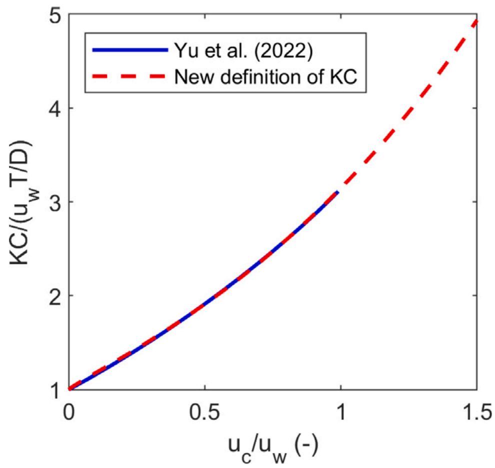

Fig. 7. Plot of the ratios between KC and u_wT/D as a function of u_c/u_w. Comparison between the definition of KC from Yu et al. (2022) and the new definition of Eq. (30).

The limit case is obtained when $u_c = u_w$, here no net zero-crossing occurs, the velocity is always positive and it is zero only at $t = 3/4T + nT$ with n positive integer. Based on this considerations, the forward and backward particle motion can be computed as:

$$A^+ = \int_{t_{u,1}}^{t_{d,1}} u(t)\,dt \qquad A^- = \int_{t_{d,1}}^{t_{u,2}} u(t)\,dt \tag{26}$$

where the zero-crossing times applied in the integration done by Yu et al. (2022) are:

$$t_{u,1} = -\frac{T}{2\pi}\arcsin\frac{u_c}{u_w} \qquad t_{d,1} = \frac{T}{2\pi}\left(\pi + \arcsin\frac{u_c}{u_w}\right) \qquad t_{u,2} = \frac{T}{2\pi}\left(2\pi - \arcsin\frac{u_c}{u_w}\right) \tag{27}$$

Therefore, two different expressions for KC, for forward and backward motion, can be obtained from Eq. (24) with the values of A as the integrals of Eq. (26). The solution was given in Yu et al. (2022) as:

$$KC^+ = \frac{u_wT}{D}\left[\left(\frac{\pi}{2} + \arcsin\frac{u_c}{u_w}\right)\frac{u_c}{u_w} + \sqrt{1-\left(\frac{u_c}{u_w}\right)^2}\right] \qquad KC^- = \frac{u_wT}{D}\left[\left(\frac{\pi}{2} - \arcsin\frac{u_c}{u_w}\right)\frac{u_c}{u_w} - \sqrt{1-\left(\frac{u_c}{u_w}\right)^2}\right] \tag{28}$$

Such expression converges to the typical definition of KC for $\frac{u_c}{u_w} \to 0$. The presence of the current increases the value of KC^+ in the forward direction up to $KC^+ = \pi u_wT/D$ for $u_c = u_w$. On the contrary, the effective value on the reverse direction KC^- decreases to zero for $u_c = u_w$.

When the current dominates the flow, a current-related value of KC_c was defined as (Yu et al., 2022):

$$KC_c = \frac{u_cT}{D} \tag{29}$$

However, Yu et al. (2022) related such parameter to the modulating effect of the waves on the current intensity. If $KC_c \ll 1$, such modulating effect is negligible, the flow is dominated by the current and it remains in almost steady conditions. Otherwise, if $KC_c \gg 1$, the wave velocity enhances the flow separation behind the obstacle.

For the purposes of the present work, the definition of KC for combined waves and currents according to Eq. (28) when $u_c \le u_w$ and to Eq. (29) when $u_c > u_w$ is characterized by some critical issues. First, a discontinuity is introduced into the model when the current velocity slightly increases from the $u_c = u_w$ case. When $u_c = u_w$, KC^+ computed with Eq. (28) is π times larger than the value computed with Eq. (29). In addition, when the current dominates the flow, it is expected for KC to go to infinity but that does not occur when applying Eq. (29). For this reasons, an exponential expression for KC is found to well represent the result of Yu et al. (2022) when the flow is wave dominated and to go to infinity for $u_w/u_c \to 0$:

$$KC = \frac{u_wT}{D}\left[-0.25 + 1.25\exp\left(\frac{u_c}{u_w}\right)^{0.87}\right] \tag{30}$$

The comparison between this new definition of KC and the expression given in Yu et al. (2022) as a function of the ratio u_c/u_w is illustrated in Fig. 7. Eq. (30) well represents the analytical expression of KC, but it extends its range of applicability to values of $u_c/u_w > 1$ and, when $u_c/u_w \to \infty$, $KC \to \infty$. The pseudocolor plot of Fig. 8 better shows the comparison between the two ways of computing KC as a function of the wave and current velocities. Fig. 8*a* highlights the criticality of the application of the approach of Yu et al. (2022), which leads to different values of KC above or behind the bisector of the u_w, u_c plane. Fig. 8*b* shows the application of Eq. (30) for the definition of KC. With respect to the results reported in Fig. 8*a*, this method does not lead to any kind of discontinuity. When a current is superimposed to a constant wave velocity, KC grows monotonically with the current velocity (see also Fig. 7). A different behaviour is obtained when the oscillatory wave velocity is added to a constant velocity field. The values of KC are always infinity when $u_w = 0$. When the wave velocity increases, the values of KC decreases tending to the wave only value of $KC_w = u_wT/D$. A further increase of the wave velocity leads to an increase of such limiting value. Therefore, for increasing wave velocity over a constant current, a minimum value of KC occurs. As an example, Fig. 9 shows the evolution of KC with u_w for fixed values of $u_c = 0.20$ m/s, $T = 8$ s and $D = 1$ m.

According to the present method and in agreement with Sumer et al. (2001), the lowest values of KC represent the most critical condition for the evaluation of the scour onset. Searching for the minimum KC through:

$$\frac{\partial KC}{\partial u_w} = 0 \tag{31}$$

gives:

$$\frac{u_w}{u_c} = \left[W(-0.23\exp -1.149) + 1.149\right]^{-1.149} \approx 0.92 \tag{32}$$

where W is the Lambert W function (Corless et al., 1996). The minimum value of KC, thus, occurs when $u_w \approx 0.92u_c$. As shown by Fig. 9, a similar behaviour is also obtained for the analytical expression of Yu et al. (2022), where the minimum value of KC is obtained for $u_w = u_c$. Also in this case, Eq. (28) can only be applied when $u_w > u_c$.

This result is also in agreement with the findings of Zang et al. (2010), who found that the largest critical velocity for the onset of scouring under combined waves and currents is approximately obtained for $\alpha = u_c/(u_c + u_w) = 0.5$.

3.3. Critical velocity

The new model for the evaluation of the scour onset through application of Eq. (13) requires the definition of the critical flow velocity under the combined action of waves and currents. When either currents or waves alone are present, the critical velocity corresponds to the current or wave velocity, respectively. If both of them exist at the same time, the critical velocity to be applied in Eq. (13) should depend on their combination, namely the parameter α defined in Eq. (6). The same approach was also used by Zang et al. (2010), where the

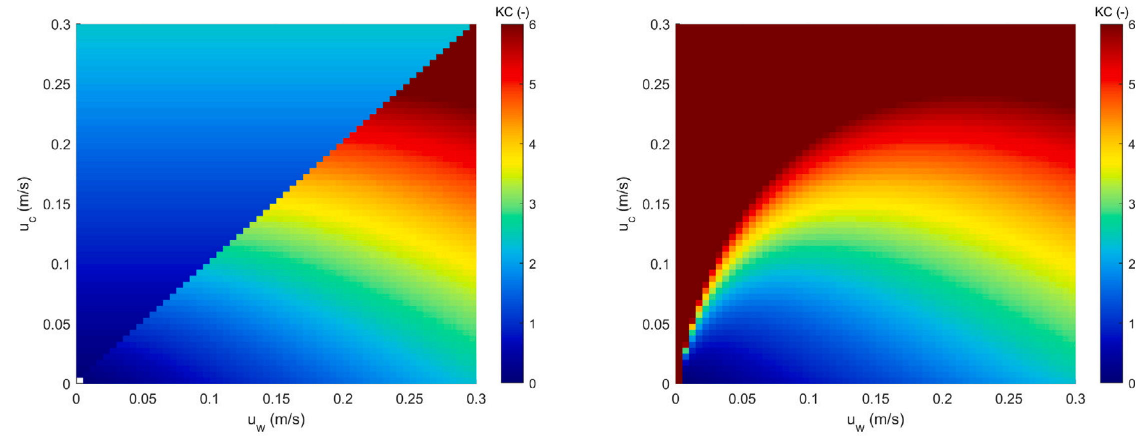

(a) (b)

Fig. 8. Evaluation of KC as a function of the wave (u_w) and current (u_c) velocity. Panel a: approach of Yu et al. (2022) with Eq. (28) for $u_w > u_c$ and with Eq. (29) for $u_w < u_c$. Panel b: new approach with Eq. (30). Results refer to $T = 8$ s and $D = 1$ m.

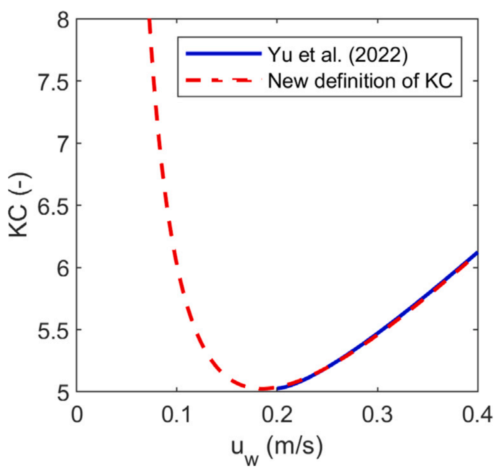

Fig. 9. Plot of KC obtained for varying values of u_w and constant values of $u_c = 0.20$, $T = 8$ s and $D = 1$ m. Comparison between the definition of KC from Yu et al. (2022) and the new definition provided in Eq. (30).

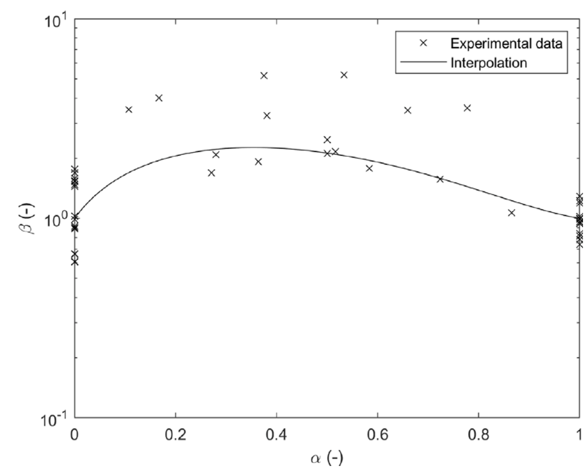

Fig. 10. Experimental data of the parameter β and plot of Eq. (35).

critical velocity was obtained by means of Eq. (5) depending on the dimensionless coefficient β. However, Eq. (7), was obtained by data fitting for application of u_{crit} on Eq. (2), only valid in current conditions. In particular, when Eq. (7) is applied to the current only case ($\alpha = 1$), a value $\beta = 0.9605 \approx 1$ is obtained and the critical velocity corresponds to the current velocity. Otherwise, for waves only conditions ($\alpha = 0$) the coefficient β becomes equal to 0.8396, thus leading to a critical velocity that is larger than the vector addition of the two velocities. For values of $0 < \alpha < 1$, $\beta > 1$ and the maximum value $\beta = 1.56$ is obtained for $\alpha = 0.52$.

The present approach is not based on the application of Eq. (5). Therefore, we here propose a different expression for β by fitting experimental data. A cubic equation for β depending on four coefficients (c_1, c_2, c_3 and c_4) has been searched for:

$$\beta(\alpha) = c_1\alpha^3 + c_2\alpha^2 + c_3\alpha + c_4 \tag{33}$$

By applying the constraints for such equation to pass through $\beta = 1$ for $\alpha = 0$ and $\alpha = 1$, Eq. (33) can be rearranged as:

$$\beta(\alpha) = c_1\alpha^3 + c_2\alpha^2 - (c_1 + c_2)\alpha + 1 \tag{34}$$

that only depends on two parameters. The experimental values of β are reported in Fig. 10. In agreement with Zang et al. (2010), β is characterized by values larger than unity when waves are combined to currents. In this work, instead of directly interpolating Eq. (34) on the experimental data, the equation for β is obtained by maximizing the r^2 value computed with the experimental and model values of Ω. The final expression for β, also reported in Fig. 10, is:

$$\beta(\alpha) = 7\alpha^3 - 15\alpha^2 + 8\alpha + 1 \tag{35}$$

According to this equation, a maximum value of $\beta = 2.26$ is obtained for $\alpha = 0.35$. Therefore, from the definition of β in Eq. (5) the critical velocity is 1.5 times smaller than the sum of the waves and current velocities. The whole method can now be applied also to the experimental results of Zang et al. (2010) and the results, in terms of the dimensionless parameter Ω, are illustrated in Fig. 11. The present method allows one to obtain a good estimate of the onset of scour conditions both in waves or currents only (Sumer et al., 2001) and in combined waves and currents (Zang et al., 2010) achieving a final value of $r^2 = 0.87$, which is equal to the coefficient of determination obtained from the application of Eq. (8), valid in steady current condition only.

4. Summary and conclusions

In the present work, a method for the evaluation of the scour onset conditions was developed based on the experimental results for only waves and current of Sumer et al. (2001) and on the results for

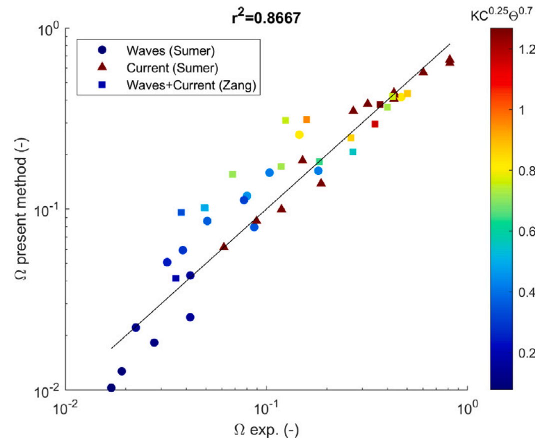

Fig. 11. Application of the present method for the evaluation of the onset of scour to the only waves or current data of Sumer et al. (2001) and to the combined waves and current data of Zang et al. (2010).

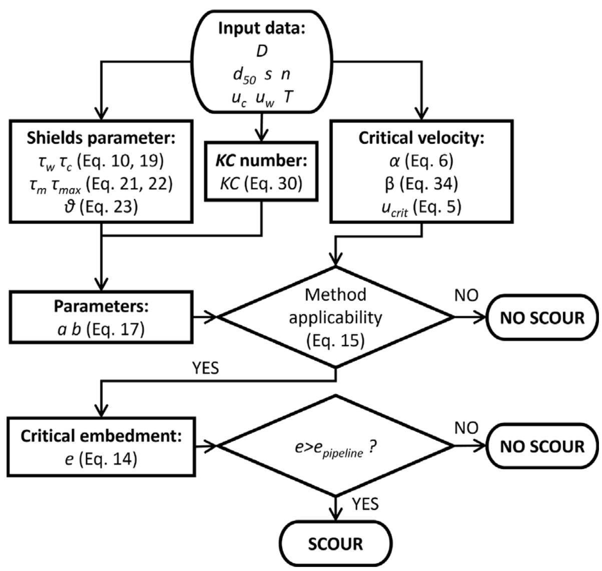

Fig. 12. Flowchart of the method for the scour onset evaluation under a pipeline in combined waves and currents.

combined waves and currents of Zang et al. (2010). Therefore, the method can be applied in waves, currents and waves plus currents conditions. The flowchart of the model is reported in Fig. 12. For its application, the following information is required:

- the pipeline diameter D;
- the soil characteristics, such as the median sediment size d_{50}, the specific weight $s = \rho_s/\rho_w$, the porosity n (it can be calculated from Eq. (16) if no information is available);
- the current velocity perpendicular to the pipeline u_c;
- the wave velocity perpendicular to the pipeline u_w and the wave period T.

Once such characteristics are known, the method can be applied through the following steps:

- compute the wave and current shear stresses, i.e. τ_w and τ_c, with Eqs. (10) and (19);
- compute the mean and maximum shear stresses, i.e. τ_m and τ_{max}, with Eqs. (21) and (22);
- compute the Shields parameter θ under combined waves and currents with Eq. (23);
- compute the KC parameter under combined waves and current with the new definition of Eq. (30);
- compute the parameters a and b with Eq. (17);
- compute α with Eq. (6);
- compute β with Eq. (35);
- compute the critical velocity u_{crit} with Eq. (5);
- check the applicability of the method with Eq. (15). If the condition is not satisfied, no scour occurs;
- compute the critical embedment of the pipeline e with Eq. (14);
- if such critical embedment is larger than the actual embedment of the pipeline, the scour onset conditions are reached.

In the development of the present method, the importance of the Shields parameter in the onset of scouring process under waves and currents is highlighted. In addition, an important parameter for waves, the KC number, was also studied. A new definition of KC was also given starting from the analytical study of Yu et al. (2022). This new definition allows for computation of KC in combined waves and currents conditions and it is in agreement with the available theoretical knowledge on wave–current interaction (e.g. Sumer and Fredsøe, 2002). The new method here proposed, allows for a good estimate of the scour onset conditions both in waves, currents or waves plus currents conditions. However, further experimental studies, focused on combined conditions, could be useful to strengthen the validation of the coefficients here obtained in the empirical equations.

CRediT authorship contribution statement

Francesco Marini: Investigation, Methodology, Validation, Writing – original draft, Writing – review & editing. **Matteo Postacchini:** Investigation, Writing – original draft, Writing – review & editing. **Claudia Pizzigalli:** Funding acquisition. **Maurizio Badalini:** Funding acquisition. **Sara Corvaro:** Supervision, Writing – review & editing. **Maurizio Brocchini:** Investigation, Project administration, Supervision.

Declaration of competing interest

The authors declare that they have no known competing financial interests or personal relationships that could have appeared to influence the work reported in this paper.

Data availability

Data will be made available on request.

Acknowledgements

The authors wish to thank the partial support provided by SAIPEM SpA.

References

Besio, G., Blondeaux, P., Brocchini, M., Vittori, G., 2003. Migrating sand waves. Ocean Dyn. 53 (3), 232–238.
Besio, G., Blondeaux, P., Brocchini, M., Vittori, G., 2004. On the modeling of sand wave migration. J. Geophys. Res.: Oceans 109 (C4).
Bijker, E., Leeuwestein, W., 1984. Interaction between pipelines and the seabed under the influence of waves and currents. In: Seabed Mechanics: Edited Proceedings of a Symposium, University of Newcastle Upon Tyne, 5–9 September, 1983. Springer, pp. 235–242.
Bijker, R., Staub, C., Silvis, F., Bruschi, R., 1991. Scour-induced free spans. In: Offshore Technology Conference. OTC, pp. OTC–6762.
Cheng, L., Yeow, K., Zang, Z., Li, F., 2014. 3D scour below pipelines under waves and combined waves and currents. Coast. Eng. 83, 137–149.
Chiew, Y.-M., 1990. Mechanics of local scour around submarine pipelines. J. Hydraul. Eng. 116 (4), 515–529.
Chiew, Y.-M., 1991. Prediction of maximum scour depth at submarine pipelines. J. Hydraul. Eng. 117 (4), 452–466.
Corless, R.M., Gonnet, G.H., Hare, D.E., Jeffrey, D.J., Knuth, D.E., 1996. On the lambert w function. Adv. Comput. Math. 5, 329–359.

Drago, M., Mattioli, M., Bruschi, R., Vitali, L., 2015. Insights on the design of free-spanning pipelines. Phil. Trans. R. Soc. A 373 (2033), 20140111. http://dx.doi.org/10.1098/rsta.2014.0111, URL: https://royalsocietypublishing.org/doi/abs/10.1098/rsta.2014.0111.

Drago, M., Pigliapoco, M., Ciuffardi, T., 2007. Analysis of pipeline fatigue damage for scour induced freespans. In: ISOPE International Ocean and Polar Engineering Conference. ISOPE, pp. ISOPE–I.

Fredsøe, J., 2016. Pipeline–seabed interaction. J. Waterw. Port Coast. Ocean Eng. 142 (6), 03116002.

Fredsoe, J., Deigaard, R., 1992. Mechanics of Coastal Sediment Transport, vol. 3, World scientific publishing company.

Grossmann, F., Hurther, D., Van der Zanden, J., Cáceres, I., Sánchez-Arcilla, A., Alsina, J.M., 2022. Near-bed sediment transport during offshore bar migration in large-scale experiments. J. Geophys. Res.: Oceans 127 (5), e2021JC017756.

Hansen, E.A., 1992. Scour below pipelines and cables, a simple model. In: Proceedings of the International Conference on Offshore Mechanics and Arctic Engineering. American Society of Mechanical Engineers, p. 133.

Keulegan, G.H., Carpenter, L.H., 1958. Forces on cylinders and plates in an oscillating fluid. J. Res. Natal. Bureau Stand. 60, 423.

Kjeldsen, S., Gjorsvik, O., Bringaker, K., Jacobsen, J., 1973. Local scour near offshore pipelines. In: Paper Available Only As Part of the Complete Proceedings of the Second International Conference on Port and Ocean Engineering under Arctic Conditions. POAC, August 27-30, 1973, pp. 308–331.

Klomp, W., Hansen, E., Chen, Z., Bijker, R., Bryndum, M., 1995. Pipeline seabed interaction, free span development. In: The Fifth International Offshore and Polar Engineering Conference, vol. All Days, OnePetro.

Liang, D., Cheng, L., 2005. A numerical model of onset of scour below offshore pipelines subject to steady currents. In: A Numerical Model of Onset of Scour Below Offshore Pipelines Subject to Steady Currents. CRC Press/Balkema, pp. 637–643.

Lucassen, R., 1984. Scour Underneath Submarine Pipelines. TU Delft, Civil Engineering and Geosciences, Hydraulic Engineering.

Mao, Y., 1986. The Interaction Between a Pipeline and an Erodible Bed (PhD Thesis). Technical University of Denmark, Lyngby, Denmark.

Melito, L., Parlagreco, L., Perugini, E., Postacchini, M., Devoti, S., Soldini, L., Zitti, G., Liberti, L., Brocchini, M., 2020. Sandbar dynamics in microtidal environments: Migration patterns in unprotected and bounded beaches. Coast. Eng. 161, 103768.

Moncada-M, A.T., Aguirre-Pe, J., 1999. Scour below pipeline in river crossings. J. Hydraul. Eng. 125 (9), 953–958.

Nikuradse, J., 1932. Gesetzmassigkeiten der turbulenten stromung in glatten rohren. Ver Deutsch. Ing. Forschungsheft 356.

Ockenden, M., Soulsby, R., 1994. Sediment Transport by Currents Plus Irregular Waves. Technical Report, HR Wallingford.

Pape, L., Plant, N., Ruessink, B., 2010. On cross-shore migration and equilibrium states of nearshore sandbars. J. Geophys. Res.: Earth Surf. 115 (F3).

Postacchini, M., Soldini, L., Lorenzoni, C., Mancinelli, A., 2017. Medium-term dynamics of a middle adriatic barred beach. Ocean Sci. 13 (5), 719–734.

Pourzangbar, A., Brocchini, M., 2022. A new process-based, wave-resolving, 2DH circulation model for the evolution of natural sand bars: The role of nearbed dynamics and suspended sediment transport. Coast. Eng. 177, 104192.

Shields, A., 1936. Anwendung der Aehnlichkeitsmechanik und der Turbulenzforschung auf die Geschiebebewegung (Ph.D. thesis). Technical University Berlin, Preussischen Versuchsanstalt für Wasserbau.

Soulsby, R., 1997. Dynamics of Marine Sands. Thomas Telford Publishing, http://dx.doi.org/10.1680/doms.25844, arXiv:https://www.icevirtuallibrary.com/doi/pdf/10.1680/doms.25844, URL: https://www.icevirtuallibrary.com/doi/abs/10.1680/doms.25844.

Soulsby, R.L., Hamm, L., Klopman, G., Myrhaug, D., Simons, R., Thomas, G., 1993. Wave-current interaction within and outside the bottom boundary layer. Coast. Eng. 21 (1–3), 41–69.

Sumer, B.M., Fredsøe, J.r., 1990. Scour below pipelines in waves. J. Waterw. Port Coast. Ocean Eng. 116 (3), 307–323.

Sumer, B.M., Fredsøe, J., 2002. The Mechanics of Scour in the Marine Environment. World Scientific, http://dx.doi.org/10.1142/4942, arXiv:https://www.worldscientific.com/doi/pdf/10.1142/4942, URL: https://www.worldscientific.com/doi/abs/10.1142/4942.

Sumer, B., Jensen, B., Fredsøe, J., 1991. Effect of a plane boundary on oscillatory flow around a circular cylinder. J. Fluid Mech. 225, 271–300.

Sumer, B.M., Truelsen, C., Sichmann, T., Fredsøe, J., 2001. Onset of scour below pipelines and self-burial. Coast. Eng. 42 (4), 313–335.

Wu, W., Wang, S.S., 2006. Formulas for sediment porosity and settling velocity. J. Hydraul. Eng. 132 (8), 858–862.

Yu, X., Rosman, J.H., Hench, J.L., 2022. Boundary layer dynamics and bottom friction in combined wave–current flows over large roughness elements. J. Fluid Mech. 931, A11.

Zang, Z., Cheng, L., Zhao, M., 2010. Onset of scour below pipeline under combined waves and current. In: International Conference on Offshore Mechanics and Arctic Engineering, vol. 49095, pp. 483–488.

Zang, Z., Cheng, L., Zhao, M., Liang, D., Teng, B., 2009. A numerical model for onset of scour below offshore pipelines. Coast. Eng. 56 (4), 458–466.

Zang, Z., Tang, G., Chen, Y., Cheng, L., Zhang, J., 2019. Predictions of the equilibrium depth and time scale of local scour below a partially buried pipeline under oblique currents and waves. Coast. Eng. 150, 94–107.

Zhang, Q., Draper, S., Cheng, L., An, H., 2017. Time scale of local scour around pipelines in current, waves, and combined waves and current. J. Hydraul. Eng. 143 (4), 04016093.

Zhang, Y., Zhang, S., Li, G., 2019. Seabed scour beneath an unburied pipeline under regular waves. Mar. Georesour. Geotechnol. 37 (10), 1247–1256.